scientific reports

Check for updates

OPEN

Transmission electron microscopy ultrastructural characteristics of the distal middle cerebral artery in moyamoya disease

Liming Zhao[1,3], Ruiyu Wu[1,3], Tao Gao[1], Yang Liu[1], Yuxue Sun[1], Gaochao Guo[1], Ziqiang Liu[1], Zhongcan Chen[1], Hugo Andrade-Barazarte[2]✉ & Chaoyue Li[1]✉

The etiology of moyamoya disease (MMD) remains unknown. The main pathological finding is fibrocellular thickening of the intima, irregular undulation of the internal elastic lamina affecting the distal portions of the internal carotid artery and A1 and M1 segments. Our aim is to describe the histological and electron microscope ultrastructural characteristics of cortical MMD vessels (middle cerebral artery) in hemorrhagic and ischemic presentation along different Suzuki stages. From January 2022 to December 2022, we collected clinical and radiological data of 310 patients with MMD, among them we identified 52 patients that underwent superficial temporal artery-middle cerebral artery (STA-MCA) bypass. We collected arterial walls (excisional arteriotomy) of the recipient arteries specifically, M3 or M4 segments of the MCA. Observations and micrographs were captured utilizing an HT7700 transmission electron microscope. MMD patients exhibit severe internal elastic lamina (IEL) changes as compared to patients with intracranial atherosclerosis. Hemorrhagic MMD presentation showed a higher score of IEL ruptured when comparing to ischemic presentation. Endothelial cells in hemorrhagic MMD showed more significant contraction compared to those in ischemic moyamoya disease. Hemorrhagic and ischemic MMD patients showed no statistically significant differences when correlated to Suzuki stages and cerebral perfusion. MMD patients exhibit IEL changes and endothelial cells contraction extending into the distal segments of the middle cerebral artery. Hemorrhagic MMD presentation has higher IEL rupture score making these patients probably more susceptible for hemorrhage. This study provides an inside of the extension of MMD into the brain surface.

Abbreviations

MMD	Moyamoya disease
ICA	Internal carotid artery
MCA	Middle cerebral artery
ACA	Anterior cerebral artery
TIA	Transient ischemic attack
CBF	Cerebral blood flow
CBV	Cerebral blood volume
STA-MCA	Superficial temporal artery to middle cerebral artery
EDMS	Encephalo-duro-myo-synangiosis
DSA	Digital subtraction angiography
TEM	Transmission electron microscope

Moyamoya disease (MMD) is a chronic occlusive cerebrovascular disease characterized by progressive stenosis of the terminal portions of the intracranial internal carotid arteries and A1 and M1 segments together with the development of collateral vessels. The etiology of the disease remains unknown[1,2]. The main pathological finding from postmorten studies have demonstrated fibrocellular thickening of the intima, irregular undulation of the internal elastic lamina and a decrease of the outer diameter of the internal carotid arteries.[1,3,4] However, while

[1]Department of Neurosurgery, Zhengzhou University People's Hospital, Henan Provincial People's Hospital, Zhengzhou, China. [2]Department of Neurosurgery, University of Toronto, Toronto Western Hospital, Toronto, Canada. [3]Liming Zhao and Ruiyu Wu contributed equally to this work. ✉email: hugo.andradebarazarte@uhn.ca; lichaoyue@zzu.edu.cn

histopathological findings in the distal middle cerebral artery have been reported in surgical specimens[4], the mechanisms and clinical implications of such distal involvement remain poorly characterized in the context of specific focus of the current study, e.g., non-surgical cohorts, radiological progression, etc.

Currently, there is growing evidence that smooth muscle proliferation is the key mechanism of the vascular occlusion in MMD[5]. Histological findings of the distal ICA have demonstrated proliferation of the smooth muscle cells or endothelium, together with neo-vascularization or hyperplasia of the intima.[1] Additionally, moyamoya vessels have shown different histological changes including fibrin deposits of the wall, fragmented elastic laminae and attenuated media. Moreover, MMD patients tend to develop cortical microvascularization in order to compensate for reduced cerebral blood flow or the aberrant active neo-vascularization before the occlusion. This is well seemed in radiological studies; however, the literature lacks on studies describing the histopathological characteristics of this vessels or segments.[6] Therefore, the aim of our study is to describe the histological and electron microscope ultrastructural characteristics of cortical MMD vessels (middle cerebral artery) in hemorrhagic and ischemic presentation as well as their correlation with different Suzuki stages which could provide an inside of the extension of MMD into the brain surface.

Methods

Study cohort

From January 2022 to December 2022, we retrospectively collected clinical and radiological data of 310 patients with MMD according to diagnosis and treatment of MMD[7] admitted at the Moyamoya Disease Research and Treatment Center of the Henan Provincial People's Hospital in Zhengzhou China.

We identified 52 patients that met the following inclusion criteria: (a) age within 14–65 years old; (b) clinical and angiographic diagnosis of MMD; (c) Complete perioperative clinical and radiological data; (d) Surgical treatment through direct superficial temporal artery to middle cerebral artery (STA-MCA) bypass + encephalo-duro-myo-synangiosis (EDMS); (e) the patient and their family members provided preoperative consent, and the informed consent form was signed. We collected MCA distal segments (excisional arteriotomy) samples of all the patients that underwent STA-MCA bypasses. Additionally, clinical data and cerebral artery wall samples were collected from 8 patients diagnosed with middle cerebral artery occlusion, constituting the control group. The general clinical data is summarized in Table 1.

Patients that failed to preclude the giving criteria and that presented with cardiopulmonary disease, hyperthyroidism, systemic lupus erythematosus, antiphospholipid antibody syndrome, peripheral arteritis, Sjogren's syndrome were excluded from the study cohort. Additionally, specimens that were too small or for other reasons cannot be embedded, sectioned, and observed were excluded as well.

This study adhered to the principles of the Helsinki Declaration and the guidelines of Good Clinical Practice, and received approval from the Ethics Committee of Henan Provincial People's Hospital (approval number: 2020183). Informed consent was obtained from each participant prior to their inclusion in the study.

Artery wall sample

We used an excisional arteriotomy to obtain part of the arterial wall of the recipient artery used for the STA-MCA anastomosis. Specifically, M3 or M4 segments of the MCA, we obtained approximately a volume greater than 1 mm^3 that was promptly immersed in EM fixative at 4 °C for 2–4 h. Following immersion, they

	MMD (n = 52)	Middle cerebral artery occlusion(n = 8)
Sex[a]		
Male	25 (48.1)	4 (50.0)
Female	27 (51.9)	4 (50.0)
Age, (years)[b]	45.33 ± 13.44	49.50 ± 10.61
Premorbid history[a]		
Hypertension	23 (41.8)	5 (55.6)
Diabetes	5 (9.1)	2 (22.2)
Smoker	12 (23.1)	2 (25.0)
Drinker	14 (26.9)	2 (25.0)
Surgical side[a]		
Left	25 (48.1)	3 (37.5)
Right	27 (51.9)	5 (62.5)
postoperative complications[a]		
Hypertransfusion	2 (3.8)	1 (12.5)
Epilepsia	4 (7.7)	1 (12.5)
Hematencephalon	4 (7.7)	–
TIA	1 (1.9)	–

Table 1. General clinical data of patients with Moyamoya disease and middle cerebral artery occlusion. [a]Percentage (%). [b]Median (Interquartile Range). [c]In this and successive tables, Suzuki stage refers to the Suzuki stage of the surgically treated side.

Suzuki classification	DSA image performance
I	Internal carotid artery stenosis, no moyamoya vessel formation
II	Small networks of blood vessels began to appear, shaped like "moyamoya"
III	The internal carotid artery was further narrowed and even began to occlude, and the moyamoya-like fine vascular network was increased
IV	The occlusion of the internal carotid artery worsened, and the otherwise dense moyamoya vessels began to decrease
V	With the further development of the IV stage, the further reduction of moyamoya vessels and increased the formation of collateral circulation in the external carotid artery
VI	Moyamoya blood vessels completely disappear, abnormal intracranial and intracranial vascular anastomosis increased, forming a new blood flow pathway to supply the blood demand of the brain

Table 2. Suzuki classification criteria.

Cerebral perfusion stages	PWI/CTP image performance
Ia	TTP was prolonged, and MTT, CBF, and CBV were normal
Ib	TTP and MTT were prolonged, with normal CBF, and normal or mildly elevated CBV
IIa	TTP, MTT was prolonged as well as CBF decreased, with essentially normal or slightly decreased CBV
IIb	TTP and MTT were prolonged, and CBF and CBV were decreased

Table 3. Cerebral perfusion stages.

underwent rinsing in a phosphate buffer (0.1 mol/L, pH 7.4), dehydration in a gradient of ethanol and 100% acetone, and embedding in tissue blocks using various proportions of EPON 812 embedding medium. Ultra-thin Sects. (60–80 nm thick) were then prepared using a UC7 diamond cutter on a Leica UC7 ultra-thin slicer. Subsequently, double staining was conducted with 2% uranium hydrogen acetate and lead citrate. Observations and micrographs were captured utilizing an HT7700 transmission electron microscope (Hitachi, Japan).

Definition of the primary observation indicator

MMD vascular progression was categorized into stages I-VI based on preoperative DSA angiography using the Suzuki grading criteria (See Table 2). The ischemic degree of MMD patients was categorized into four levels (Ia, Ib, IIa, and IIb) based on preoperative CTP/PWI examination according to the Gao Peiyi criteria. (See Table 3).

The intimal layer primarily consists of vascular endothelial cells and the internal elastic membrane, which significantly impact vessel wall integrity and stability. We used ImageJ 1.54 g(URL: http://imagej.org), a processing software to measure the area of endothelial cells under a 3000 × transmission electron microscope to analyze cell morphology and shrinkage. Additionally, we observed the internal elastic membrane at 1000 × magnification and assign value scores: no break (0 points), mild break (< 3 breaks, 1 point), moderate break (< 5 breaks, 2 points), severe break (5 breaks, 3 points).

Samples were screened for processing artifacts prior to analysis. Regions with mechanical tears were excluded; only zones with intact morphology underwent IEL assessment.

Statistics

Data analysis was conducted using GraphPad Prism8.0.2.263 (URL: https://www.graphpad.com/) statistical software. Continuous variables not following a normal distribution are presented as M (Q1, Q3), with the Mann–Whitney U test for two-group comparisons and the Kruskal–Wallis test for multiple-group comparisons; categorical variables are reported as counts (percentages or composition ratios). A significance level of $P < 0.05$ was used to determine statistical significance.

Results

Characteristics of cortical arteries in moyamoya disease and intracranial middle cerebral artery occlusion through TEM

Ultrastructural characteristics (Table 4, Fig. 1)

(a) *Intima* Vascular endothelial cells (Enc) exhibit varying degrees of edema, necrosis, and shedding in MMD. The internal elastic lamina (IEL) shows waviness, visible thinning, and rupture. Smooth muscle cells (SMC) abundantly were observed in the intimal layer. Irregular nuclear morphology with a heterochromatin border is noted, along with varying numbers of mitochondria and dilated endoplasmic reticulum.

Patients with middle cerebral artery occlusion exhibit cortical vascular endothelial cells and organelle edema, along with folding of the IEL, reminiscent of a "sandwich-like" alteration, smooth muscle cells are visible in the interstitium. Irregularities are observed in the nuclear morphology and heterochromatin borders of endothelial cells. Additionally, there are indications of mitochondria swelling and dilated endoplasmic reticulum.

Ultrastructure	MMD (n = 52)	Middle cerebral artery occlusion (n = 8)
Tunica intima		
Endothelial cell	Pyknosis, necrosis, and shedding	Edema
Basement membranae	Incrassation	Same
Internal elastic lamina	Break	"Sandwich-like" alteration
Nucleus	Heterochromatin border	Same
Mitochondria	Variable quantity	Rich in quantity
Rough endoplasmic reticulum	Eclasis	Same
Smooth muscle cell migration	More	Few
Tunica media		
Smooth muscle cell	Abundant, edema	Same
Nucleus	Heterochromatin border	Same
Mitochondria	Few	More
Rough endoplasmic reticulum	Eclasis	Same
Dense patches and dense bodies	Variable quantity	Depletion in numbers
Adventitia		
Fibroblasts	Collapse, necrosis	Same
Nucleus	Scarce	Complete
Mitochondria	Dissolve, disappear	Same
Rough endoplasmic reticulum	Dissolve, disappear	Same
Collagen Fibers	Abundant	Same

Table 4. Ultrastructural observations of brain surface vessels in patients with moyamoya disease and middle cerebral artery occlusion.

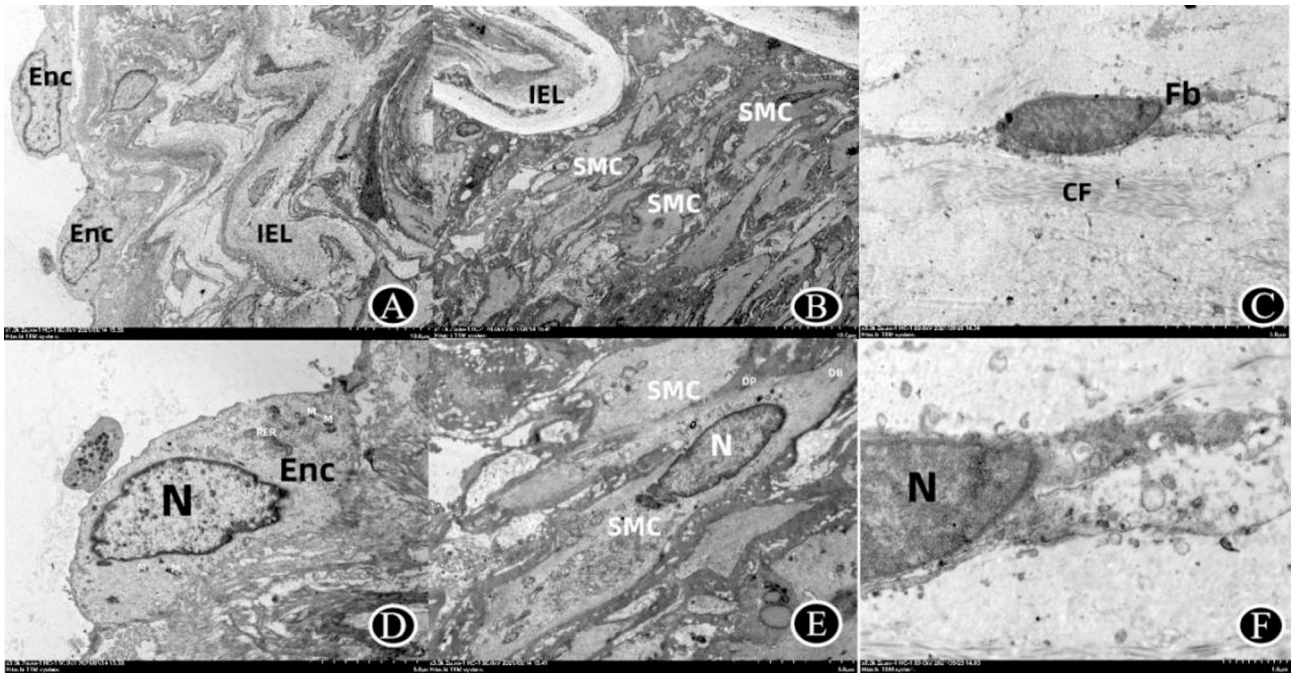

Fig. 1. Typical picture of TEM results of internal carotid artery occlusion (D-F is local magnification of A-C). A (X1000 times) Internal elastic lamina tear, "sandwich-like" changes, migration of a few smooth muscle cells to the intimal layer, swelling of endothelial cells with irregular nuclei and heterochromatin edge setting; abundant mitochondria showing swelling, light matrix, reduced or disappeared cristae; and dilation of rough endoplasmic reticulum. B (X3000 times) shows abundant smooth muscle cells with intact cell membranes, fewer organelles, elongated spindle nuclei, clear nuclear membranes, heterochromatin edge setting, and a small number of dense patches and dense bodies evenly distributed. C (X3000 times) reveals necrotic fibroblasts with disintegrated and free organelles, intact nuclei, and abundant collagen filaments surrounding the cells. IEL: Internal elastic lamina; Enc: endothelial cells; N: nucleus; M: mitochondria: RER: rough endoplasmic reticulum; SMC:smooth muscle cell; DP:dense patches; DB: dense body;Fb:Fibroblasts; CF: collagen filament.

(b) *Media* In MMD, abundant smooth muscle cells were visible on the surface of the artery. The majority of nuclei displayed an elongated spindle shape, while the density of both dense patches (DP) and dense bodies (DB) within plaques varies. Patients with middle cerebral artery occlusion showed an abundance of smooth muscle cells with a diffuse arrangement. The nuclei were oval, containing abundant mitochondria, with a reduced density of dense bodies and dense patches.
(c) *Adventitia* In MMD, there is notable fibroblast disintegration, scattered organelles, and abundant collagen fibers (CF) surrounding the cells. Patients with middle cerebral artery occlusion displayed fibroblasts edema, disintegration, organelle dissolution, and disappearance on the brain's surface, along with abundant collagen fibers surrounding the cells.

Differential variability of IEL and Enc in MMD and middle cerebral artery occlusion

(1) The alterations in the elastic membrane on the brain surface in MMD ([M(Q1, Q3) = 2 (2,3)]) and MCA occlusion ([M(Q1, Q3) = 0 (0,0)]) were statistically significant ($P < 0.001$).The severity of internal elastic membrane changes in MMD patients exceeded that in patients with middle cerebral artery occlusion (Table 5, Fig. 2).
(2) The area of vascular endothelial cells on the brain surface was assessed for MMD ([M(Q1,Q3) = 15.81(7.87, 22.65)μm^2]) and middle cerebral artery occlusion ([M(Q1,Q3) = 30.19(16.07,58.92)μm^2]), indicating a statistically significant difference ($P = 0.002$). (Table 5, Fig. 2).

Characteristics of cortical arteries in ischemic and hemorrhagic MMD

Ultrastructural observations: (Table 6, Figs. 3 and 4)

(a) *Intima* the majority of vascular endothelial cells of hemorrhagic MMD patients showed necrosis and detachment, while the IEL appears wavy, thin, and ruptured. Many smooth muscle cells were seen in the intimal layer, while endothelial cell nuclei exhibit irregular morphology, heterochromatin borders, variable mitochondria, and dilated endoplasmic reticulum.

In ischemic MMD, vascular endothelial cells exhibit varying degrees of edema, necrosis, and shedding similar to hemorrhagic MMD. The IEL shows waviness, visible thinning, and discontinuity. Smooth muscle cells abundantly migrate to the intimal layer. Irregular nuclear morphology with a heterochromatin border is noted, along with varying numbers of mitochondria and dilated endoplasmic reticulum.

(b) *Media* In hemorrhagic and ischemic moyamoya disease, abundant smooth muscle cells are observable on the surface of cerebral blood vessels. The majority of the nuclei displayed an elongated spindle shape, while the density of both DP and DB within the plaques varies.
(c) *Adventitia* In hemorrhagic and ischemic moyamoya disease, there is significant fibroblast disintegration, scattered organelles, and abundant collagen fibers surrounding the cells.

Differential variability of IEL and Enc in hemorrhagic and ischemic MMD

(1) The score of IEL rupture in hemorrhagic ([M(Q1, Q3) = 2 (1,3)]) and ischemic MMD [M(Q1, Q3) = 1 (0,2)]), showed a statistically significant difference ($P = 0.013$), suggesting a notably higher incidence of internal elastic lamina injury in patients with hemorrhagic presentation (Table 7, Figs. 3 and 4).
(2) The area of vascular endothelial cells were statistically difference in hemorrhagic MMD ([M(Q1,Q3) = 12.68 (1.08,20.90) μm^2]) ([M(Q1,Q3) = 16.42 (10.20,23.36) μm^2]) ($P = 0.046$). Endothelial cells in hemorrhagic MMD showed significant contraction compared to those in ischemic MMD (Table 7, Figs. 3 and 4).

Characteristics of hemorrhagic MMD according to Suzuki grading

Ultrastructural characteristics (Table 8)

(a) *Intima* As Suzuki stage progresses, structural damage to vascular Enc, basal membrane(BM), and IEL tends to worsen, while changes in cell nucleui, mitochondria, rough endoplasmic reticulum (ER), and smooth muscle cell migration remain consistently throughout the Suzuki stages.
(b) *Media* Along the different Suzuki stages, vascular smooth muscle cells remain abundant, exhibiting swelling and irregular changes in their nuclei. Meanwhile, mitochondria decreases, and rough ER expands. The

	IEL		Enc	
	Number	Value scores[a]	Number	Area(um^2)[a]
MMD	52	2 (2, 3)	81	15.81 (7.87, 22.65)
Middle Cerebral Artery occlusion	8	0 (0, 0)	8	30.19 (16.07, 58.92)
P-value		< 0.001*		0.002*

Table 5. Comparative analysis of the endothelial cell area and Internal Elastic Iamina break of the brain surface vessels in patients with moyamoya disease and middle cerebral artery occlusion. [a]M(Q_1, Q_3), *$P < 0.05$.

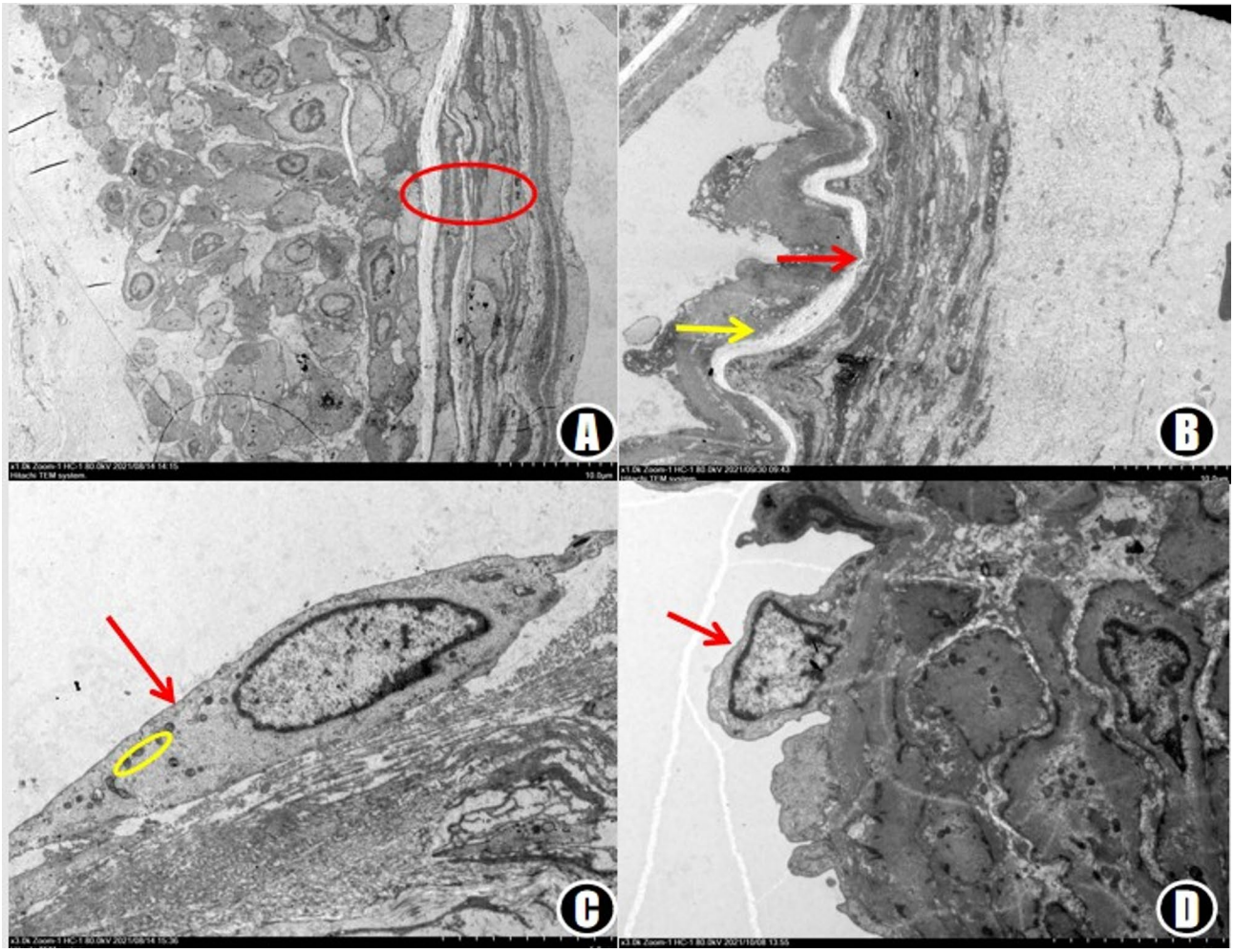

Fig. 2. A (X1000 times) The internal elastic lamina of the internal carotid artery occlusion was curved and torn, with a "sandwich" -like change (red area). B (X1000 times) The internal elastic lamina of moyamoya disease cortex is wavy (yellow arrow), with local thinning and fracture (red arrow). C(X3000 times) The endothelial cells of the internal carotid artery had long spindle shape, irregular nucleus shape, heterochromatin edge set, mitochondria (yellow area) were rich, swollen, matrix became light, and the crest part disappeared. D (X3000 times) The vascular endothelial cells of moyamoya disease cortex are irregular shaped (red arrow), the nucleus is irregular, heterochromatin edge set, with a small amount of mitochondria and swelling.

number of DP decreases in Suzuki II and III stages, and increases in Suzuki IV and V. The quantity of DB decreases in Suzuki II, then increases in Suzuki III-IV, and decreases in stage V.

(c) *Adventitia* During the Suzuki stage progression, no significant changes were observed in the outer layer. There was evidence of disintegration and necrosis of fibroblasts, the presence of scattered organelles, a blurred structure, and abundant collagen fibers surrounding the cells.

Differential variability of IEL and Enc in different Suzuki stages of hemorrhagic moyamoya disease

(1) The score of IEL rupture on the brain surface was assessed for hemorrhagic MMD at Suzuki stages II(0.00), Suzuki stage III ([M(Q1,Q3) = 2.00(1.25,2.75)]), Suzuki stage IV ([M(Q1,Q3) = 2.00(1.00,3.00)]), and Suzuki stage V ([M(Q1,Q3) = 1.50(1.00,2.00)]), showing no statistically significant difference ($P = 0.293$).(Table 9, Fig. 5).

(2) The area of vascular endothelial cells on the brain surface was evaluated for hemorrhagic MMD at Suzuki stage II (19.22 μm^2), Suzuki III ([M(Q1,Q3) = 13.84(2.76,18.1) μm^2]), Suzuki IV ([M(Q1,Q3) = 15.23(6.23,22.89) μm^2]), and Suzuki V ([M(Q1,Q3) = 1.039(0.00,7.025) μm^2]), showing no statistically significant difference ($P = 0.235$). However, compared to Suzuki stages II-IV, the endothelial cell area in phase V showed significant reduction (Table 9, Fig. 5).

Ultrastructure	Ischemic MMD (n = 33)	Hemorrhagic MMD (n = 19)
Tunica intima		
Endothelial cell	Pyknosis and shedding	Obvious pyknosis and shedding
Basement membranae	Incrassation	Same
Internal elastic lamina	Thin, broken	Same
Nucleus	Heterochromatin border	Same
Mitochondria	Swelling, break of the cristae	Same
Rough endoplasmic reticulum	Eclasis	Same
Smooth muscle cell migration	More	Same
Tunica media		
Smooth muscle cell	Abundant, edema	Same
Nucleus	Heterochromatin border	Same
Mitochondria	Swelling, break of the cristae	Same
Rough endoplasmic reticulum	Eclasis, degranulation	Same
Dense patches and dense bodies	Variable quantity	Depletion in numbers
Adventitia		
Fibroblasts	Collapse, necrosis	Same
Nucleus	scarce	Same
Mitochondria	Scarce, pyknosis	Same
Rough endoplasmic reticulum	Dissolve, disappear	Same
Collagen fibers	Abundant	Same

Table 6. Common observation of ultrastructure of brain surface vessels in hemorrhagic and ischemic MMD.

Characteristics of ischemic MMD according to Suzuki grading

Ultrastructural characteristics (Table 10)

(a) *Intima* Swelling, pyknosis, and necrosis of endothelial cells are common across different Suzuki stages, with insignificant ultrastructural changes; smooth muscle cell migration occurs throughout all Suzuki stages.
(b) *Media* Smooth muscle cells were abundant across various Suzuki stages, exhibiting swelling, pyknosis, and necrosis features. The organelle count was notably decreased, resulting in a blurred structure. DP and DB are plentiful and evenly dispersed.
(c) *Adventitia* During the Suzuki stage progression, no significant changes were observed in the outer layer. There was evidence of disintegration and necrosis of fibroblasts, the presence of scattered organelles, a blurred structure, and abundant collagen fibers surrounding the cells.

Differential variability of IEL and Enc in different Suzuki stages of ischemic moyamoya disease

(1) The score of IEL rupture for ischemic MMD at Suzuki stage II ([M(Q1,Q3) = 0.50(0.00,3.00)]), Suzuki stage III ([M(Q1,Q3) = 1.00(0.00,1.00)]), Suzuki stage IV ([M(Q1,Q3) = 1.00(0.75,2.00)]), and stage V ([M(Q1,Q3) = 1.00(1.00,1.00)]), showed no statistically significant difference ($P = 0.886$).(Table 11, Fig. 6).
(2) The area of vascular endothelial cells for ischemic MMD at Suzuki stages II ([M(Q1,Q3) = 16.68(6.01,27.44) μm^2]), III ([M(Q1,Q3) = 16.45(11.19,24.23) μm^2]), IV ([M(Q1,Q3) = 15.19(10.20,23.96) μm^2]), and V ([M(Q1,Q3) = 18.36(17.99,18.74) μm^2]), showed no statistically significant difference ($P = 0.957$).(Tables 11, 12, and 13 Fig. 6).

Characteristics of hemorrhagic and ischemic MMD correlated to cerebral perfusion deficits

Ultrastructural characteristics (Tables 12 and 14)

(a) *Intima* ischemic and hemorrhagic presentation exhibited swelling, shedding, pyknosis, and necrosis of endothelial cells across various cerebral perfusion stages, with no significant ultrastructural changes observed. Smooth muscle cell migration occurred consistently during the cerebral perfusion stage.
(b) *Media* Hemorrhagic and ischemic MMD samples showed smooth muscle cells in varying numbers across different cerebral perfusion stages, exhibiting characteristics such as swelling, pyknosis, and necrosis. Mitochondria exhibited swelling, while the quantity of DP and DB varied. There was no significant difference between the presentations when correlated to cerebral perfusion.
(c) *Adventitia* different degrees of cerebral perfusion impairment showed no significant changes in the outer layer. Ischemic and hemorrhagic MMD presentations showed disintegration and necrosis of fibroblasts, presence of scattered organelles, a blurred structure, and abundant collagen fibers surrounding the cells. No significant difference between the presentations when correlated to cerebral perfusion.

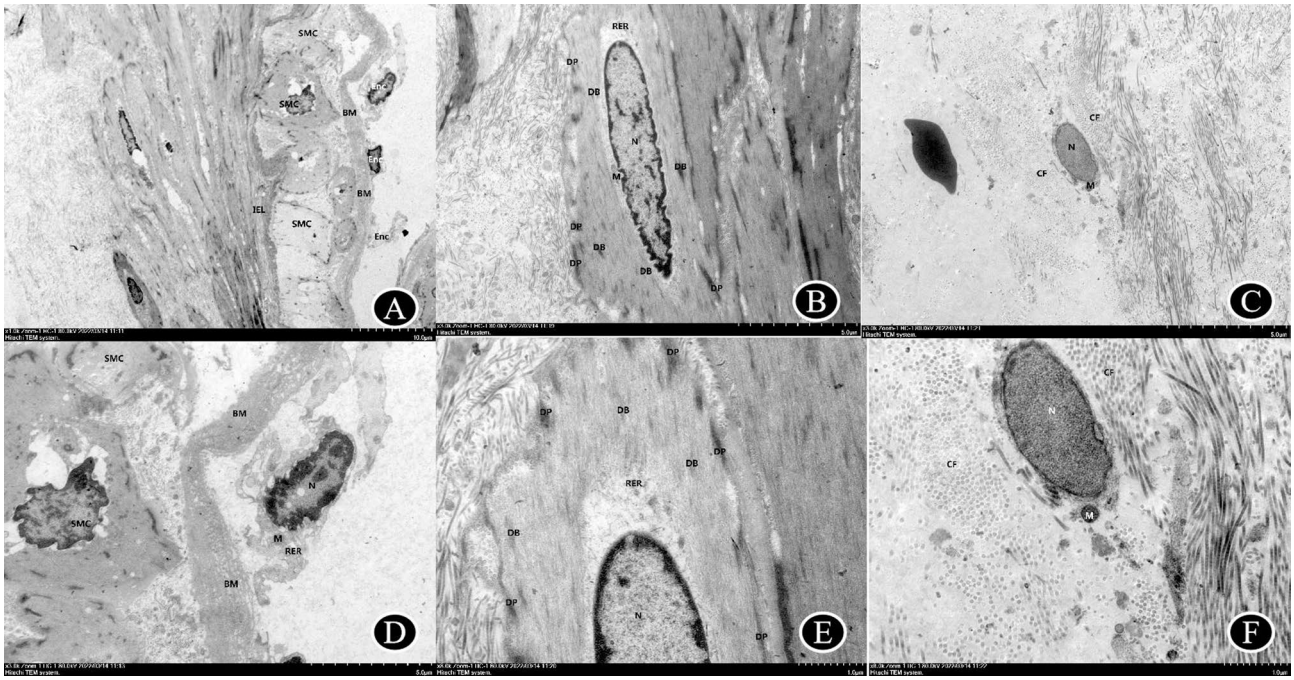

Fig. 3. Typical picture of TEM results of hemorrhagic MMD(D-F is local magnification of A-C). A (X1000 times) The internal elastic lamina is discontinuous and local residual, more smooth muscle cells migrating to the inner membrane layer. Endothelial cells were mostly shed and free, exhibiting damaged cell membranes, irregular nuclei, without obvious mitochondrial swelling, and with rough endoplasmic reticulum expansion. The basement membrane was sparse and notably thickened. B (X3000 times) Smooth muscle cells are neatly arranged with slightly enlarged intercellular gaps. The cells exhibit relatively regular nuclear morphology, clear and intact nuclear membranes with defined heterochromatin, few organelles, uniform mitochondrial matrix, thick endoplasmic reticulum showing membrane dissolution, and abundance. The local dense spot is significantly longer, and the number of dense bodies is more abundant. C (X3000 times) Fibroblasts are disintegrated, necrotic, and fragmented with disappeared cell membranes. There are abundant collagen filaments around the cells, irregular nuclei, fixed contraction, increased heterochromatin, uneven chromatin, and disappearance of other organelle structures. IEL: internal elastic lamina; BM: basement membranae;Enc: endothelial cells; N: nucleus; M: mitochondria: RER: rough endoplasmic reticulum; SMC: smooth muscle cell; DP:dense patches; DB: dense body;Fb:Fibroblasts; CF: collagen filament.

Differential variability of IEL and Enc in different cerebral perfusion stages of hemorrhagic and ischemic MMD (Tables 13 and 15, Figs. 7 and 8)

(1) The score of IEL rupture for hemorrhagic MMD was at Cerebral perfusion Ib([M(Q1,Q3) = 2.00(1.50,2.50)]), at IIa ([M(Q1,Q3) = 1.00(0.25,2.50)]) and IIb ([M(Q1,Q3) = 2.00(1.00,3.00)]), showing no statistically significant difference ($P = 0.496$).(Table 13, Fig. 7). The score of IEL rupture for ischemic MMD at Cerebral perfusion Ib ([M(Q1,Q3) = 0.50(0.00,1.75)]), IIa ([M(Q1,Q3) = 1.50(01.00,2.00)]) and IIb ([M(Q1,Q3) = 1.00(0.00,1.00)]), showing no statistically significant difference ($P = 0.097$).(Table 15, Fig. 8).
(2) The area of vascular endothelial cells in hemorrhagic MMD was at Cerebral perfusion Ib ([M(Q1,Q3) = 11.99(2.20,16.32) μm^2]), IIa ([M(Q1,Q3) = 5.63(1.06,19.64) μm^2]), and IIb ([M(Q1,Q3) = 16.06(0.00,24.54) μm^2]), showing no statistically significant difference ($P = 0.591$). (Table 13, Fig. 7). Similar the area of vascular endothelial cells in ischemic MMD was at Cerebral perfusion Ib ([M(Q1,Q3) = 25.28(7.08,30.16) μm^2]), IIa ([M(Q1,Q3) = 15.79(10.09,19.32) μm^2]) and IIb ([M(Q1,Q3) = 16.04(10.78,21.11) μm^2]), showing no statistically significant difference ($P = 0.375$).(Table 15, Fig. 8).

Discussion

Moyamoya disease (MMD) is a rare and chronic occlusive cerebrovascular disease characterized by the excessive proliferation of vascular endothelial cells or smooth muscle cells. The main pathological finding in MMD patients is fibrocellular thickening of the intima, irregular undulation of the internal elastic lamina and decrease of the outer diameter of the internal carotid arteries. However, its extension into the distal segments of the middle cerebral artery has not been described.

Moreover, identifying vascular structural changes could help to elucidate the pathogenesis of moyamoya disease, making it an ideal subject for research. In this study, we used a TEM to observe the ultrastructural changes of the brain surface blood vessels of MMD patients.

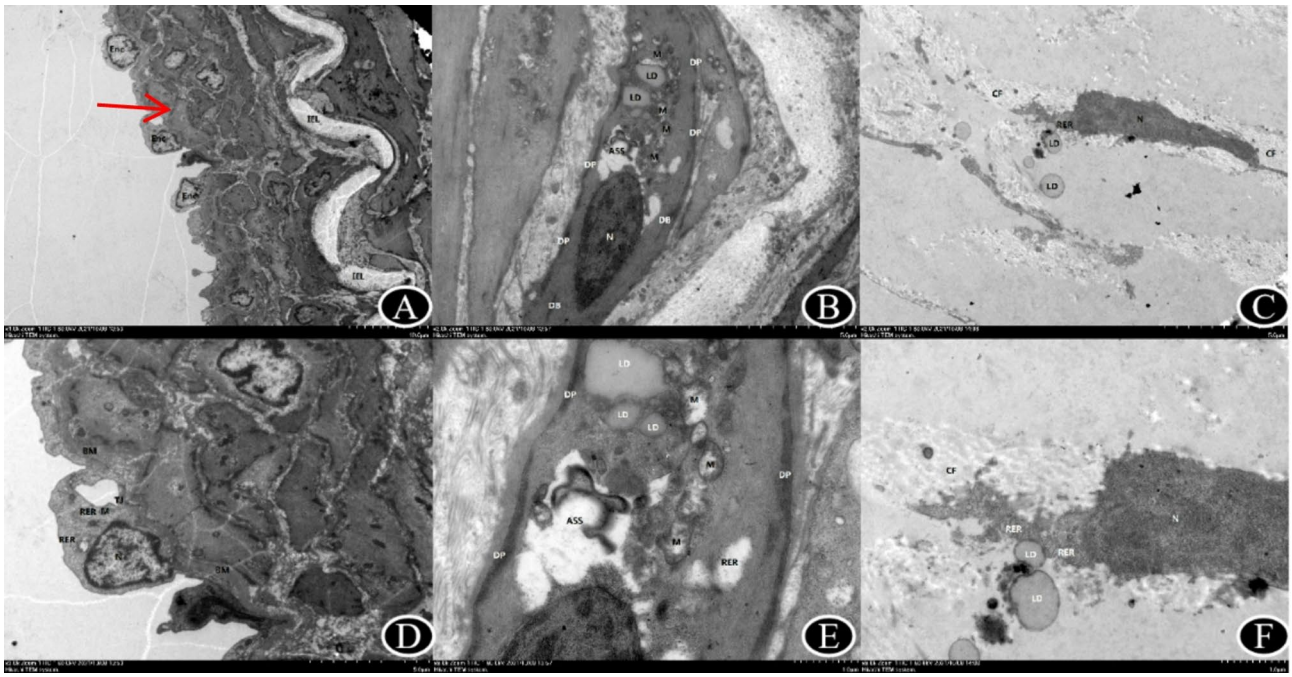

Fig. 4. Typical picture of TEM results of ischemic MMD(D-F is local magnification of A-C). A (X1000 times) The internal elastic lamina has uneven thickness, local rupture, and massive migration of smooth muscle cells to the intimal layer more smooth muscle cells migrating to the inner membrane layer(red arrow). Endothelial cells have mild hyperplasia, with fair cell matrix, irregular nucleus and slightly swollen mitochondria, shallow matrix and slightly broken crest, and slight expansion of rough endoplasmic reticulum. The basement membrane is locally sparse and mildly thickened. B (X3000 times) Smooth muscle cells are long spindle shape, mild swollen, large, regular arrangement and fair intercellular spaces. The nucleus is spindle shaped, not widened, heterochromatin increases and edge set; mitochondria is relatively abundant, mostly swollen, uneven matrix, broken, shorter and reduced, and a few membranes are damaged; rough endoplasmic reticulum is expanded and membrane is damaged; dense spot is significantly longer and increased, and the number of dense body is small and evenly distributed. C (X3000 times) Fibroblasts are disintegrated, necrotic, and fragmented with disappeared cell membranes. There are abundant collagen filaments around the cells, irregular nuclei, fixed contraction, increased heterochromatin, uneven chromatin, and disappearance of other organelle structures. IEL: internal elastic lamina; BM: basement membranae;Enc: endothelial cells; N: nucleus; M: mitochondria: RER: rough endoplasmic reticulum; SMC: smooth muscle cell; DP:dense patches; DB: dense body;Fb:Fibroblasts; CF: collagen filament.

Variable	IEL		Enc	
	Number	Value scores[a]	Number	Area(um^2)[a]
Hemorrhagic MMD	19	2 (1, 3)	27	12.68 (1.08, 20.90)
Ischemic MMD	33	1 (0, 2)	54	16.42 (10.20, 23.36)
P-value		0.013*		0.046*

Table 7. Comparative analysis of the endothelial cell area and Internal Elastic Iamina break of the brain surface vessels in patients with hemorrhagic and ischemic MMD. [a]M(Q_1, Q_3), *$P < 0.05$.

Endothelial cells changes

Endothelial cells constitute the crucial component of the vascular intima, acting as a semi-permeable barrier separating blood circulation from organ tissues[8]. Being metabolically active, the endothelium plays an indispensable role in maintaining various aspects of vascular homeostasis. Upon exposure to environmental changes, endothelial cells release various signaling molecules, including prostacyclin, endothelin, and endothelium-derived relaxation factors, to communicate with neighboring cells[9,10]. This process helps maintain blood vessel integrity and regulates key physiological functions such as membrane permeability, lipid transport, vasomotor tension, coagulation, and inflammation[11,12]. Nevertheless, chronic injury and degeneration lead to the loss of replication capacity in endothelial cells, resulting in subendothelial exposure, disrupted vascular integrity, increased fragility, and a heightened risk of vascular rupture and bleeding[13]. In this study, we observed edema, necrosis, and pyknosis in endothelial cells in moyamoya disease. Intracranial atherosclerosis patients showed only edema in endothelial cells. Endothelial cells from MMD patients exhibited more pronounced pyknosis.

Ultrastructure	Suzuki stage			
	II (n = 1)	III (n = 4)	IV (n = 10)	V(n = 4)
Tunica intima				
Endothelial cell	Complete	Few shedding	More shedding	More shedding
Basement membranae	Break	Incrassation	Ditto	Ditto
Internal elastic lamina	continuation	continuation	Thin, broken	Thin, broken
Nucleus	Heterochromatin border	Ditto	Ditto	Disappear
Mitochondria	Swelling, break of the cristae	Ditto	Ditto	Disappear
Rough endoplasmic reticulum	Eclasis	Ditto	Ditto	Ditto
Smooth muscle cell migration	–	Abundant	Ditto	Ditto
Tunica media				
Smooth muscle cell	Complete	Abundant,edema	Same	Same
Nucleus	Heterochromatin border	Ditto	Ditto	Ditto
Mitochondria	Disappear	Swelling, break of the cristae	Ditto	Ditto
Rough endoplasmic reticulum	Eclasis	Ditto	Ditto	Ditto
Dense patches and dense bodies	Depletion in numbers	Dense Patches decreases;Dense Bodies are abundant	Dense Patches increases;Dense Bodies are abundant	Dense Patches increases;Dense Bodies are decreases
Adventitia				
Fibroblasts	Collapse, necrosis	Ditto	Ditto	Ditto
Nucleus	–	Few, damage and disintegration	Ditto	Ditto
Mitochondria	–	Scarce, pyknosis	Ditto	Ditto
Rough endoplasmic reticulum	Disappear	Ditto	Ditto	Ditto
Collagen fibers	Abundant	Ditto	Ditto	Ditto

Table 8. Common observation of ultrastructural observations of brain surface vessels in different Suzuki stages of hemorrhagic moyamoya disease.

Variable	IEL		Enc	
	Number	Value scores[a]	Number	Area(um^2)[a]
Suzuki stage[b]				
II	1	0[c]	1	19.22[c]
III	4	2.00 (1.25, 2.75)	6	13.84 (2.76, 18.14)
IV	10	2.00 (1.00, 3.00)	14	15.23 (6.23, 22.89)
V	4	1.50 (1.00, 2.00)	6	1.039 (0.00, 7.025)
P-value		0.293		0.235

Table 9. Comparative analysis of the endothelial cell area and Internal Elastic Iamina break of the brain surface vessels in different Suzuki stages of hemorrhagic moyamoya disease. [a] M(Q1,Q3). [b] In this and successive tables, Suzuki stage refers to the Suzuki stage of the surgically treated side.[c] $^{*}P < 0.05$.

Studies suggest that endothelial cell shedding and pyknosis may be caused by inflammatory infiltration and oxidative stress on the vascular wall[14,15]. Inflammation leads to the release of cytokines and chemical mediators, which can damage the structure and function of endothelial cells. Additionally, oxygen free radicals and other oxidative molecules can also damage endothelial cells, resulting in their shedding or pyknoid changes. The exclusive presence of EC necrosis in MMD (vs. ICAS) may reflect chronic hemodynamic stress and oxidative damage in stenotic vessels, compounded by defective vascular repair mechanisms. In contrast, edema in ICAS likely stems from transient inflammatory insults without irreversible membrane damage. Our findings of endothelial damage and IEL disruption align with mechanistic studies implicating RNF213 mutations in vascular fragility. Then the fragility of moyamoya vessels is closely linked to their defective architecture, which predisposes them to rupture under hemodynamic stress[16]. The p.R4810K variant has been shown to impair endothelial cell migration and promote smooth muscle cell apoptosis, processes that could exacerbate mural thinning and collateral vessel instability[17,18]. Furthermore, RNF213 dysfunction may disrupt oxidative stress responses, rendering vessels prone to hemodynamic injury. Although this study lacked genetic genotyping data, the observed pathological changes align with RNF213-associated vascular pathogenesis, suggesting that genetic background may be a critical factor influencing endothelial damage in MMD. Future work correlating RNF213 status with ultrastructural pathology could clarify its role in IEL degradation and hemorrhagic transformation.

Our study identified a higher pyknosis of endothelial cells in the surface vessels of hemorrhagic moyamoya disease as compared to ischemic presentation. Clinical studies have indeed demonstrated a higher risk of

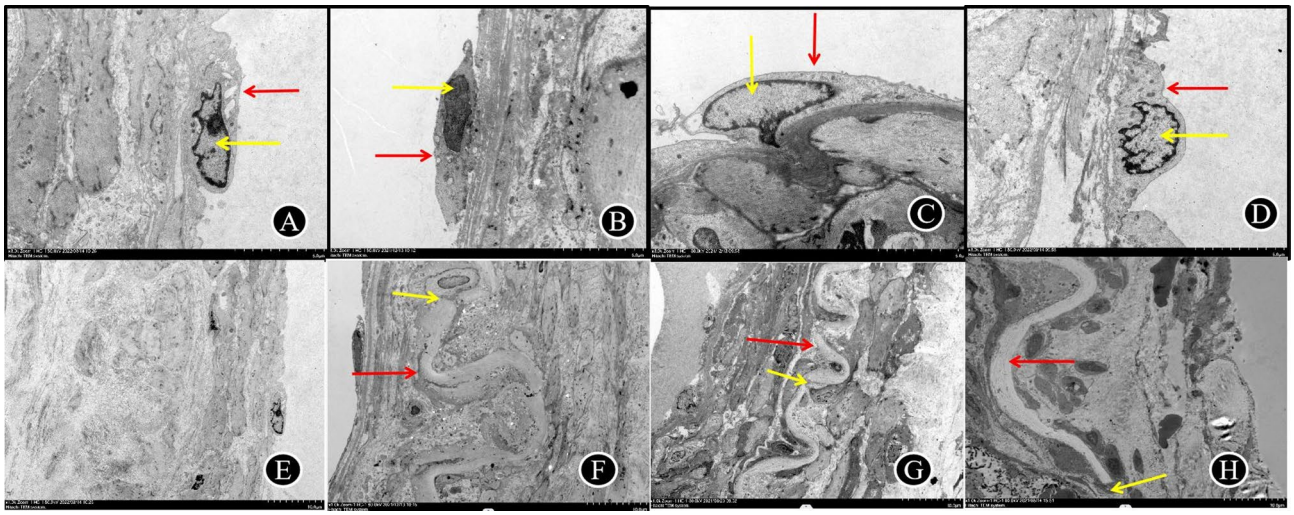

Fig. 5. A–D vascular endothelial cells of hemorrhagic MMD (red arrow) are long spindle shape, complete cell membrane, irregular nucleus (yellow arrow), heterochromatin border.With the Suzuki stage, endothelial cells became pyknosis and necrosis increased; E–H the internal elastic lamina (red arrow) in hemorrhagic MMD was wavy, and the thinning and fracture (yellow arrow) worsened with the progression of Suzuki stage.(A and E:Suzuki II stage; B and F:Suzuki III stage; C and G:Suzuki IV stage; D and H: Suzuki V stage).

Ultrastructure	Suzuki stage			
	II (n = 6)	III (n = 7)	IV (n = 18)	V (n = 2)
Tunica intima				
Endothelial cell	Pyknosis,necrosis, and shedding	Ditto	Ditto	Ditto
Basement membranae	Incrassation	Ditto	Ditto	Ditto
Internal elastic lamina	Thin, break	Ditto	Ditto	Ditto
Nucleus	Heterochromatin border	Ditto	Ditto	Ditto
Mitochondria	Swelling, break of the cristae	Ditto	Ditto	Ditto
Rough endoplasmic reticulum	Eclasis	Ditto	Ditto	Ditto
Smooth muscle cell migration	More	Ditto	Ditto	Ditto
Tunica media		Ditto	Ditto	Ditto
Smooth muscle cell	swelling	Ditto	Ditto	Ditto
Nucleus	Heterochromatin border	Ditto	Ditto	Ditto
Mitochondria	Swelling, break of the cristae	Ditto	Ditto	Ditto
Rough endoplasmic reticulum	Eclasis	Ditto	Ditto	Ditto
Dense patches and dense bodies	Equally distributed	Ditto	Ditto	Ditto
Adventitia				
Fibroblasts	Collapse, necrosis	Ditto	Ditto	Ditto
Nucleus	A small amount of residual	Ditto	Ditto	Ditto
Mitochondria	Scarce, swelling	Ditto	Ditto	Ditto
Rough endoplasmic reticulum	Eclasis	Ditto	Ditto	Ditto
Collagen fibers	Abundant	Ditto	Ditto	Ditto

Table 10. Common observation of ultrastructural observations of brain surface vessels in different Suzuki stages of ischemic moyamoya disease.

mortality and rebleeding in hemorrhagic MMD, with a poorer prognosis[19,20]. The reported cumulative risk of rebleeding over 5, 10, 15, and 19 years was 7.8%, 22.6%, 35.9%, and 19.1% respectively, indicating a progressive increase in the risk of rebleeding among patients with hemorrhagic MMD over time[21].

Additionally, the shedding and disappearance of endothelial cells in the vascular wall of moyamoya disease have become common phenomena. As the Suzuki stage progresses, the shedding and disappearance of endothelial cells worsen in hemorrhagic moyamoya disease, whereas no significant difference is observed in ischemic moyamoya disease. This suggests a lack of positive correlation between Suzuki stage, cerebral perfusion stage, and the severity of moyamoya disease.

variable	IEL		Enc	
	Number	Value scores[a]	Number	Area(um^2)[a]
Suzuki stages[b]				
II	6	0.50 (0, 3.00)	8	16.68 (6.01, 27.44)
III	7	1.00 (0, 1.00)	14	16.45 (11.19, 24.23)
IV	18	1.00 (0.75, 2.00)	30	15.19 (10.20, 23.96)
V	2	1.00 (1.00, 1.00)	2	18.36 (17.99, 18.74)
P-value		0.886		0.957

Table 11. Comparative analysis of the endothelial cell area and Internal Elastic Iamina break of the brain surface vessels in different Suzuki stages of ischemic moyamoya disease. [a]M(Q1,Q3). [b] this and successive tables, Suzuki stage refers to the Suzuki stage of the surgically treated side. *$P < 0.05$.

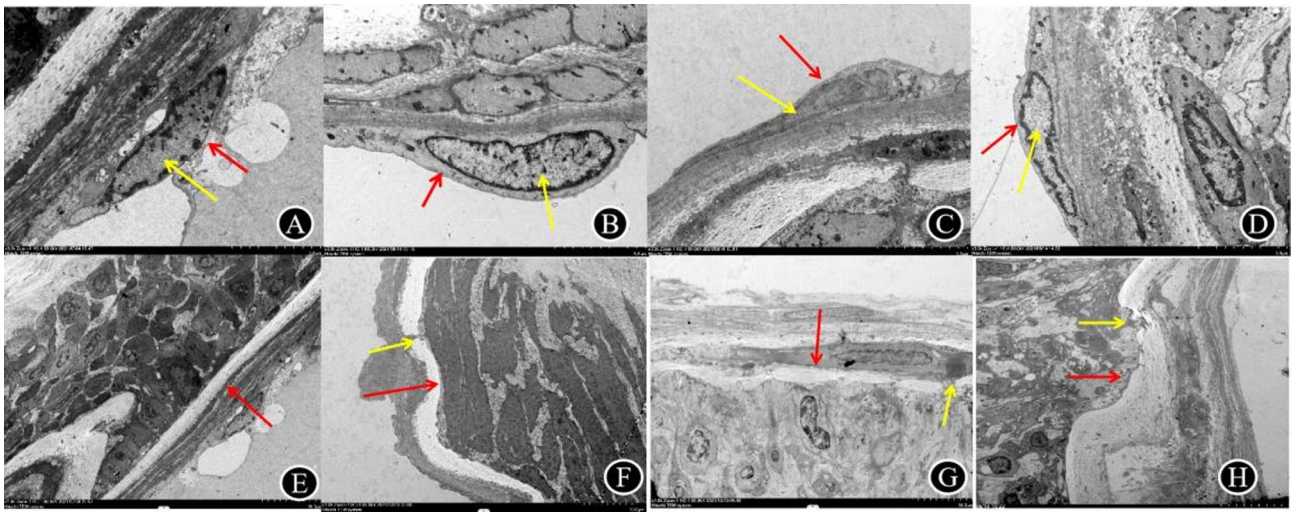

Fig. 6. A–D vascular endothelial cells of ischemic MMD (red arrow) are long spindle shape, complete cell membrane, irregular nucleus (yellow arrow), heterochromatin border.There was no significant difference in the different Suzuki stages ; E–H the internal elastic lamina (red arrow) in ischemic MMD was wavy, with local thin fracture (yellow arrow) and no obvious difference under different Suzuki stages.(A and E:Suzuki II stage; B and F:Suzuki III stage; C and G:Suzuki IV stage; D and H: Suzuki V stage).

Internal elastic lamina findings

The internal elastic lamina is a vital component of the intimal layer, consisting of elastic fibers that are highly elastic and tough. It plays various roles such as maintaining vascular structure, regulating tone, decreasing blood flow resistance, promoting platelet aggregation, and contributing to vascular repair.[22,23] Atherosclerosis, inflammation, trauma, and other factors can diminish the IEL, reducing its elasticity and potentially causing disruption[24,25]. Our study showed that in moyamoya disease, the IEL on the cerebral surface primarily exhibited tearing and rupture, whereas in patients with middle cerebral artery occlusion, the IEL changes were predominantly "sandwich"-like. These differences may partly elucidate the distinct developmental mechanisms for both diseases.

IEL damage in hemorrhagic MMD is significantly more critical than in ischemic moyamoya disease. This difference may be attributed to hemorrhagic MMD ability to induce greater elastase secretion, resulting in severe vascular damage. IEL rupture could also contribute to bleeding. It is noteworthy that as the Suzuki stage or cerebral perfusion stages advances, it tends to be a worsening of IEL rupture in the MCA of hemorrhagic Moyamoya disease. Despite the lack of statistical significance ($P > 0.05$), there was still a trend towards progressive aggravation of the disease. Hence, early diagnosis and treatment are crucial for patients with moyamoya disease.

Media changes

The MCA media layer primarily involve the migration of smooth muscle cells and alterations in the dense patches and dense bodies of the cytoskeletal system. Smooth muscle cell migration and the movement of these cells to the intimal layer, plays a crucial role in maintaining the vascular structure, and aiding in vascular remodeling and repair, as well as participating in the inflammatory response.

The migration of smooth muscle cells is influenced by growth factors, cytokines, mechanical stress, and other factors. Additionally, diseases like atherosclerosis and vasculitis also impact this process[26–29]. When SMCs

Ultrastructure	cerebral perfusion stage		
	Ib (n = 5)	IIa (n = 4)	IIb (n = 10)
Tunica intima			
Endothelial cell	Pyknosis,necrosis, and shedding	Same	Same
Basement membranae	Incrassation	Same	Same
Internal elastic lamina	Thin, continuation	Thin, break	Same
Nucleus	Heterochromatin border	Same	Same
Mitochondria	Swelling, break of the cristae	Same	Same
Rough endoplasmic reticulum	Eclasis	Same	Same
Smooth muscle cell migration	More	Same	Same
Tunica media			
Smooth muscle cell	swelling	Same	Same
Nucleus	Heterochromatin border	Same	Same
Mitochondria	Swelling, break of the cristae	Same	Same
Rough endoplasmic reticulum	Eclasis	Same	Same
Dense patches and Dense bodies	Equally distributed	Same	Same
Adventitia			
Fibroblasts	Collapse, necrosis	Same	Same
Nucleus	A small amount of residual	Same	Same
Mitochondria	disappear	Same	Same
Rough endoplasmic reticulum	A small amount of residual	Same	Same
Collagen fibers	Abundant	Same	Same

Table 12. Common observation of ultrastructure of cerebral surface vessels in different cerebral perfusion stages of hemorrhagic moyamoya disease.

Variable	IEL		Enc	
	Number	Value scores[a]	Number	Area (um^2)[a]
Cerebral perfusion stage[b]				
Ib	5	2.00 (1.50, 2.50)	7	11.99 (2.20, 16.32)
IIa	4	1.00 (0.25, 2.50)	6	5.63 (1.06, 19.64)
IIb	10	2.00 (1.00, 3.00)	14	16.06 (0.00, 24.54)
P-value		0.496		0.591

Table 13. Comparative analysis of the endothelial cell area and Internal Elastic Iamina break of the brain surface vessels in different cerebral perfusion stage of hemorrhagic moyamoya disease. [a]M(Q1,Q3). [b]In this and successive tables, cerebral perfusion stage refers to the cerebral perfusion stage of the surgically treated side. $^{*}P < 0.05$.

migrate and proliferate in the media, new thickened intimal layers developed, participating as a key factor in vascular restenosis and plays a prominent role in the pathological process of intimal hyperplasia[30].

After the vascular intima is damaged, multiple cytokines and chemokines are upregulated at various time points and in different types of vascular cells. This triggers a complex series of biological responses that promote the proliferation of the vascular intima[28,30]. This study reveals that vascular smooth muscle cell migration in MMD is more pronounced than in internal carotid artery occlusion. Through analysis of moyamoya disease patients across different Suzuki stages and cerebral perfusion stages, we observed a significant migration of smooth muscle cells into the intima, while the media retained a high density of smooth muscle cells.

DP and DB play crucial roles in the cytoskeletal system of vascular smooth muscle cells. The DP can sense signals from outside the cell and transmit them inside, triggering the contraction of smooth muscle cells; meanwhile, DB regulate intracellular calcium ion concentrations, thereby influencing the contraction and relaxation of smooth muscle cells. This study observed a decrease in DP and DB on the brain surface vessels in intracranial atherosclerosis. Whereas, there was an initial decrease followed by an increase in DP, and an initial increase followed by a decrease in DB in hemorrhagic Moyamoya disease vessels. DP and DB ischemic MMD vessels were abundant and evenly distributed. A decrease in DP and an increase in DB may indicate smooth muscle cells in a contracted state, while an increase in DB and a decrease in DP may suggest smooth muscle cells undergoing proliferation or migration. This indicates that the vascular wall cell skeleton system in ischemic moyamoya disease is relatively stable compared to that in hemorrhagic moyamoya disease, reducing its susceptibility to bleeding events.

Ultrastructure	Cerebral perfusion stage		
	Ib (n = 9)	IIa (n = 8)	IIb (n = 16)
Tunica intima			
Endothelial cell	Pyknosis,necrosis, and shedding	Same	Same
Basement membranae	Incrassation	Same	Same
Internal elastic lamina	Thin, break	Same	Same
Nucleus	Heterochromatin border	Same	Same
Mitochondria	Swelling, break of the cristae	Same	Same
Rough endoplasmic reticulum	Eclasis	Same	Same
Smooth muscle cell migration	A certain amount	Same	Same
Tunica media			
Smooth muscle cell	swelling	Same	Same
Nucleus	Heterochromatin border	Same	Same
Mitochondria	Swelling, break of the cristae	Same	Same
Rough endoplasmic reticulum	Eclasis	Same	Same
Dense patches and dense bodies	Many	Depletion in numbers	Depletion in numbers
Adventitia			
Fibroblasts	Collapse, necrosis	Same	Same
Nucleus	A small amount of residual	Same	Same
Mitochondria	disappear	Same	Same
Rough endoplasmic reticulum	A small amount of residual	Same	Same
Collagen Fibers	Abundant	Same	Same

Table 14. Common observation of ultrastructure of cerebral surface vessels in different cerebral perfusion stages of ischemic moyamoya disease.

Variable	IEL		Enc	
	Number	Value scores[a]	Number	Area(um^2)[a]
Cerebral perfusion stage[b]				
Ib	8	0.50 (0.00, 1.75)	13	25.28 (7.08, 30.16)
IIa	8	1.50 (1.00, 2.00)	17	15.79 (10.09, 19.32)
IIb	17	1.00 (0.00, 1.00)	24	16.04 (10.78, 21.11)
P-value		0.097		0.375

Table 15. Comparative analysis of the endothelial cell area and Internal Elastic Iamina break of the brain surface vessels in different cerebral perfusion stage of ischemic moyamoya disease. [a]M(Q1,Q3). [b]In this and successive tables, cerebral perfusion stage refers to the cerebral perfusion stage of the surgically treated side. $^{*}P < 0.05$.

Adventitia changes

The adventitia, the outermost connective tissue of blood vessels, supports vessel protection and regulates their structure and function. Fibroblasts, crucial components of the adventitia, can influence the functional and structural aspects of the tunica intima and media through phenotypic changes such as proliferation, migration, and differentiation, among others[31,32]. Recent studies suggest that remodeling precedes the intima and media layers, making the outside-to-inside hypothesis a focal point of research[33]. Abundant fibroblast disintegration, organelle dispersion, and pericellular collagen fiber richness were observed in the MCA of middle cerebral artery occlusion and various Suzuki stages and types of MMD. This indicates a vascular injury process from the outer to the inner layers in MMD and middle cerebral artery occlusion.

Cell organelles, including the nucleus, mitochondria, endoplasmic reticulum, Golgi apparatus, and lysosomes, play diverse roles across various cellular locations and types, collectively contributing to the maintenance of normal blood vessel function[22,34].. In this study, we observed irregular nuclei and heterochromatic at the edges of the endothelial cells and smooth muscle cells nucleus in MMD and middle cerebral artery occlusion, suggesting a continuous renewal and differentiation phenomenon during vascular injury.

Conclusion

MMD patients exhibit ultrastructural changes affecting the distal segments of the MCA. There are ultrastructural differences between MMD and ICAO which helps to understand their pathophysiological processes. Hemorrhagic MMD presentation has higher IEL rupture score making these patients probably more susceptible for hemorrhage. The endothelial cells and IEL of hemorrhagic and ischemic MMD exhibit differences, that

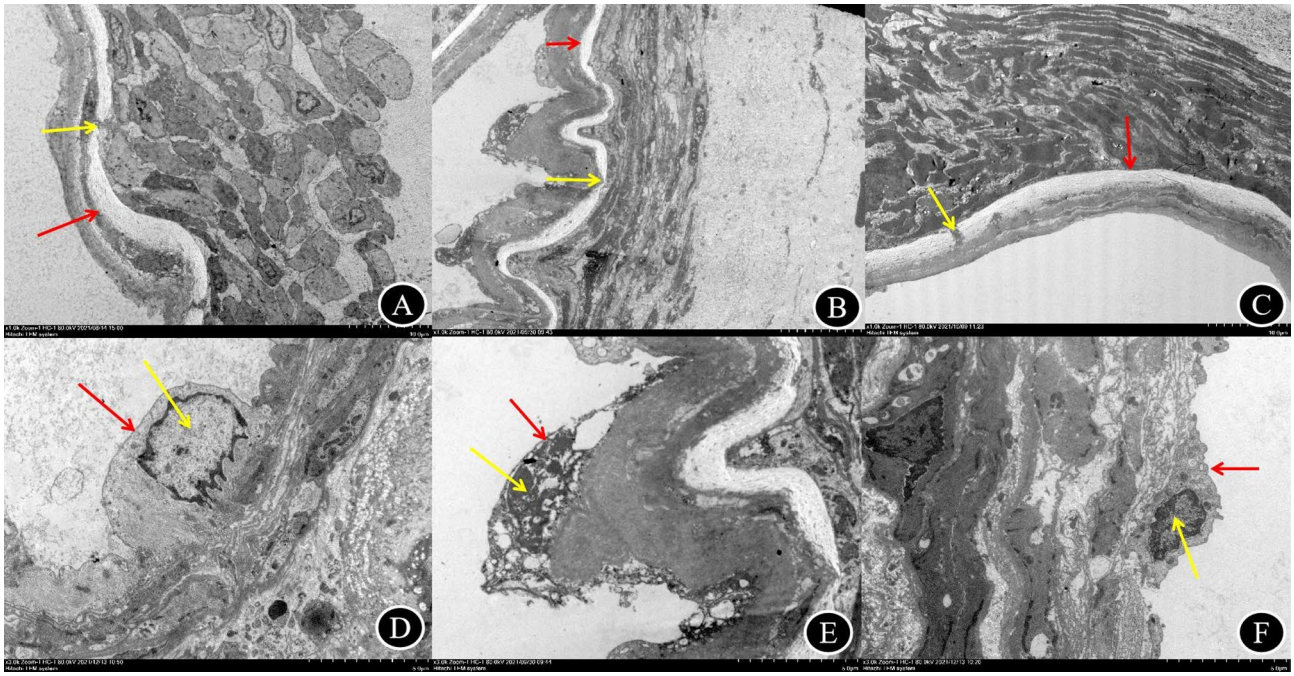

Fig. 7. A-C The internal elastic lamina (red arrow) in hemorrhagic MMD was wavy, with local thin fracture (yellow arrow) and no obvious difference in different Cerebral perfusion stages; D-F vascular endothelial cells of hemorrhagic MMD (red arrow) are long spindle shape, complete cell membrane, irregular nucleus (yellow arrow), heterochromatin border.There was no significant difference in the different Cerebral perfusion stages .(A and D:Cerebral perfusion Ib stages ; B and E:Cerebral perfusion IIa stages; C and F:Cerebral perfusion IIb stages).

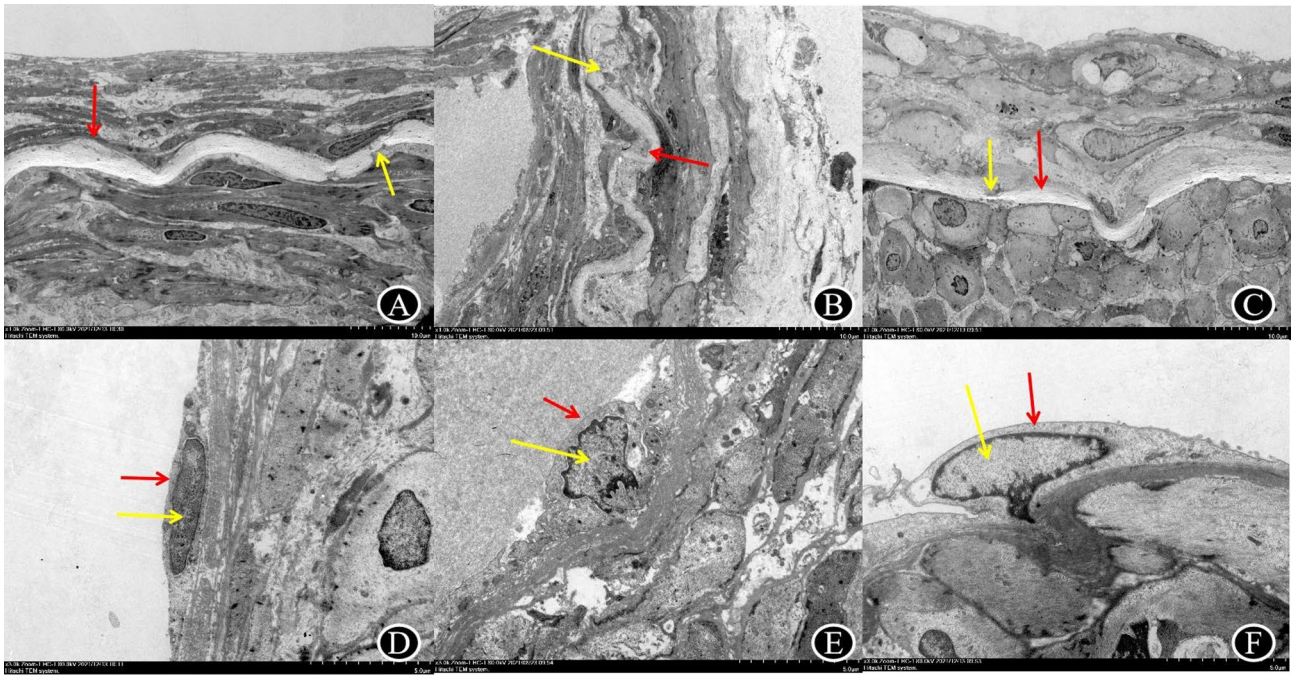

Fig. 8. A–C The internal elastic lamina (red arrow) in ischemic MMD was wavy, with local thin fracture (yellow arrow) and no obvious difference in different Cerebral perfusion stages; D-F vascular endothelial cells of ischemic MMD (red arrow) are long spindle shape, complete cell membrane, irregular nucleus (yellow arrow), heterochromatin border.There was no significant difference in different Cerebral perfusion stages. (A and D:Cerebral perfusion Ib stages; B and E:Cerebral perfusion IIa stages; C and F:Cerebral perfusion IIb stages).

might correlate to their clinical presentation, therefore laying a foundation for further research to understand the disease.

Limitations

This study has several limitations. First, angiographic evaluation strictly adhered to the Suzuki classification system, which is designed for anterior circulation pathology. Due to incomplete posterior circulation imaging data (e.g., missing vertebral artery injection sequences), we were unable to systematically assess the degree of posterior communicating artery (PCA) stenosis or leptomeningeal collateral compensation patterns. This gap may hinder a comprehensive interpretation of the pathological mechanisms underlying distal cortical vascular changes. Second, while advanced three-dimensional ultrastructural imaging (e.g., focused ion beam-scanning electron microscopy) and AI-driven organelle segmentation tools now enable quantitative analysis of organelle spatial dynamics, this study was limited to conventional histopathological techniques. Consequently, subcellular pathological features such as mitochondria-ER microdomain interactions in the vascular walls of Moyamoya disease (MMD) could not be elucidated. Finally, the absence of molecular data on the RNF213 gene—particularly the p.R4810K variant—precluded an exploration of the association between genetic susceptibility and ultrastructural vascular phenotypes (e.g., basement membrane thickening, smooth muscle cell apoptosis). This limits our ability to interpret the gene-environment interactions driving vascular fragility in MMD. Future multicenter studies should integrate quantitative posterior circulation staging, ultra-high-resolution microscopic imaging, and multi-omics profiling to establish a more comprehensive genotype–phenotype framework for MMD.

Data availability

The datasets used and/or analyzed during the current study are available from the corresponding author upon reasonable request.

Received: 19 January 2025; Accepted: 24 June 2025
Published online: 05 August 2025

References

1. Kuroda, S. & Houkin, K. Moyamoya disease: Current concepts and future perspectives. *Lancet Neurol.* **7**(11), 1056–1066. https://doi.org/10.1016/S1474-4422(08)70240-0 (2008).
2. Demartini, Z. et al. Moyamoya disease and syndrome: A review. *Radiol. Bras.* **55**(1), 31–37. https://doi.org/10.1590/0100-3984.2021.0010 (2022).
3. Reid, A. J. et al. Diffuse and uncontrolled vascular smooth muscle cell proliferation in rapidly progressing pediatric moyamoya disease. *J. Neurosurg-Pediatr.* **6**(3), 244–249. https://doi.org/10.3171/2010.5.PEDS09505 (2010).
4. Takagi, Y. et al. Histological features of middle cerebral arteries from patients treated for Moyamoya disease. *Neurol med-Chir.* **47**(1), 1–4. https://doi.org/10.2176/nmc.47.1 (2007).
5. Guo, D. C. et al. Mutations in smooth muscle alpha-actin (ACTA2) cause coronary artery disease, stroke, and Moyamoya disease, along with thoracic aortic disease. *Am. J. Hum. Genet.* **84**(5), 617–627. https://doi.org/10.1016/j.ajhg.2009.04.007 (2009).
6. Mugikura, S., Fujimura, M. & Takahashi, S. Cortical microvascularization and leptomeningeal collaterals in moyamoya disease. *Eur. Neurol.* **73**(5–6), 351–352. https://doi.org/10.1159/000430811 (2015).
7. Kuroda, S. et al. Diagnostic criteria for moyamoya disease - 2021 revised version. *Neurol. Med. Chir (Tokyo)* **62**(7), 307–312. https://doi.org/10.2176/jns-nmc.2022-0072 (2022).
8. Esper, R. J. et al. Endothelial dysfunction: A comprehensive appraisal. *Cardiovasc. Diabetol.* **5**, 1. https://doi.org/10.1186/1475-2840-5-4 (2006).
9. McCreary, D. D. et al. Survey of the extracellular matrix architecture across the rat arterial tree. *JVS Vasc. Sci.* **3**, 1–14. https://doi.org/10.1016/j.jvssci.2021.08.001 (2021).
10. Xu, S. et al. Transcriptomic profiling of intracranial arteries in adult patients with moyamoya disease reveals novel insights into its pathogenesis. *Front. Mol. Neurosci.* **15**, 881954. https://doi.org/10.3389/fnmol.2022.881954 (2022).
11. Baspinar, O. et al. Osteopontin as an early predictor of atherosclerosis in attack-free Familial Mediterranean fever patients. *Medicine* **102**(39), e35137. https://doi.org/10.1097/MD.0000000000035137 (2023).
12. Corrado, E. et al. Endothelial dysfunction and carotid lesions are strong predictors of clinical events in patients with early stages of atherosclerosis: A 24-month follow-up study. *Coronary Artery Dis.* **19**(3), 139–144. https://doi.org/10.1097/MCA.0b013e3282f3fbde (2008).
13. Giannotta, M., Trani, M. & Dejana, E. VE-cadherin and endothelial adherens junctions: Active guardians of vascular integrity. *Dev. Cell* **26**(5), 441–454. https://doi.org/10.1016/j.devcel.2013.08.020 (2013).
14. Rengarajan, A. et al. Immune cells and inflammatory mediators cause endothelial dysfunction in a vascular microphysiological system. *Lab. Chip.* **24**(6), 1808–1820. https://doi.org/10.1039/d3lc00824j (2024).
15. Cefalo, C. M. A. et al. Endothelial dysfunction is associated with reduced myocardial mechano-energetic efficiency in drug-naïve hypertensive individuals. *Intern. Emerg. Med.* **18**(8), 2223–2230. https://doi.org/10.1007/s11739-023-03402-9 (2023).
16. Funaki, T. et al. Angiographic features of hemorrhagic moyamoya disease with high recurrence risk: A supplementary analysis of the Japan Adult Moyamoya Trial. *J. Neurosurg.* **128**(3), 777–784. https://doi.org/10.3171/2016.11.JNS161650 (2018).
17. Morimoto, T. et al. Significant association of the RNF213 p.R4810K polymorphism with quasi-moyamoya disease. *J. Stroke Cerebrovasc. Dis.* **25**(11), 2632–2636. https://doi.org/10.1016/j.jstrokecerebrovasdis.2016.07.004 (2016).
18. Tinelli, F. et al. Vascular remodeling in moyamoya angiopathy: From peripheral blood mononuclear cells to endothelial cells. *Int. J. Mol. Sci.* **21**(16), 5763. https://doi.org/10.3390/ijms21165763 (2020).
19. Kobayashi, E. et al. Long-term natural history of hemorrhagic moyamoya disease in 42 patients. *J. Neurosurg.* **93**(6), 976–980. https://doi.org/10.3171/jns.2000.93.6.0976 (2000).
20. Kuroda, S. et al. Incidence and clinical features of disease progression in adult moyamoya disease. *Stroke* **36**(10), 2148–2153. https://doi.org/10.1161/01.STR.0000182256.32489.99 (2005).
21. Kang, S. et al. Natural course of moyamoya disease in patients with prior hemorrhagic stroke. *Stroke* **50**(5), 1060–1066. https://doi.org/10.1161/STROKEAHA.118.022771 (2019).
22. Perrotta, I. The microscopic anatomy of endothelial cells in human atherosclerosis: Focus on ER and mitochondria. *J. Anat.* **237**(6), 1015–1025. https://doi.org/10.1111/joa.13281 (2020).

23. Ding, S. et al. The downstream network of STAT6 in promoting vascular smooth muscle cell phenotypic switch and neointimal formation. *Cell Biol. Int.* **47**(9), 1573–1588. https://doi.org/10.1002/cbin.12056 (2023).
24. Sarrat-Torres, R. et al. Peculiarities of the parietal organisation of the superficial temporal artery. *Rev. Neurologia* **36**(11), 1022–1025 (2003).
25. Farand, P., Garon, A. & Plante, G. E. Structure of large arteries: Orientation of elastin in rabbit aortic internal elastic lamina and in the elastic lamellae of aortic media. *Microvasc. Res.* **73**(2), 95–99. https://doi.org/10.1016/j.mvr.2006.10.005 (2006).
26. Yuan, W. et al. Effects of BMSCs interactions with adventitial fibroblasts in transdifferentiation and ultrastructure processes. *Int. J. Clin. Exp. Pathol.* **7**(7), 3957–3965 (2014).
27. Tahir, H. et al. An in silico study on the role of smooth muscle cell migration in neointimal formation after coronary stenting. *J. R. Soc. Interface* **12**(108), 20150358. https://doi.org/10.1098/rsif.2015.0358 (2015).
28. Kundumani-Sridharan, V. et al. Nuclear factor of activated T cells c1 mediates p21-activated kinase 1 activation in the modulation of chemokine-induced human aortic smooth muscle cell F-actin stress fiber formation, migration, and proliferation and injury-induced vascular wall remodeling. *J. Biol. Chem.* **288**(30), 22150–22162. https://doi.org/10.1074/jbc.M113.454082 (2013).
29. Roy-Chaudhury, P. et al. Cellular phenotypes in human stenotic lesions from haemodialysis vascular access. *Nephrol. Dial. Transpl.* **24**(9), 2786–2791. https://doi.org/10.1093/ndt/gfn708 (2009).
30. Sharma, M. et al. Stromal-derived factor-1/CXCR4 signaling: Indispensable role in homing and engraftment of hematopoietic stem cells in bone marrow. *Stem Cells Dev.* **20**(6), 933–946. https://doi.org/10.1089/scd.2010.0263 (2011).
31. Tinajero, M. G. & Gotlieb, A. I. Recent developments in vascular adventitial pathobiology: The dynamic adventitia as a complex regulator of vascular disease. *Am. J. Pathol.* **190**(3), 520–534. https://doi.org/10.1016/j.ajpath.2019.10.021 (2019).
32. Huertas, A. et al. Chronic inflammation within the vascular wall in pulmonary arterial hypertension: More than a spectator. *Cardiovasc. Res.* **116**(5), 885–893. https://doi.org/10.1093/cvr/cvz308 (2020).
33. Stenmark, K. R. et al. The adventitia: Essential regulator of vascular wall structure and function. *Annu. Rev. Physiol.* **75**, 23–47. https://doi.org/10.1146/annurev-physiol-030212-183802 (2012).
34. Stacchiotti, A. et al. Mitochondrial and metabolic dysfunction in renal convoluted tubules of obese mice: Protective role of melatonin. *PLoS ONE* **9**(10), e111141. https://doi.org/10.1371/journal.pone.0111141 (2014).

Author contributions

All authors contributed to the study conception and design. Material preparation, data collection and analysis were performed by Liming Zhao, Ruiyu Wu, Ziqiang Liu and Gaochao Guo. The first draft of the manuscript was written by Liming Zhao and Ruiyu Wu. Tao Gao, Yang Liu, Yuxue Sun and Zhongcan Chen drafted the work or revised it critically for important intellectual content. Hugo Andrade-Barazarte and Chaoyue Li drafted the work or revised it critically for important intellectual content and approved the version to be published and agree to be accountable for all aspects of the work in ensuring that questions related to the accuracy or integrity of any part of the work are appropriately investigated and resolved. All authors read and approved the final manuscript.

Funding

Henan Provincial Leading Talents Project Fund for Young and Middle-aged Health and Health Technology in 2021 (YXKC2021004); Henan Province Key Research and Development and Promotion Special Science and Technology Tackle Key Project Fund (222102310046); Jointly Constructed Project Fund of Henan Medical Science and Technology Tackle Key Project (LHGJ20220025).

Declarations

Competing interests

The authors declare no competing interests.

Ethical approval

This study received approval from the Ethics Committee of Henan Provincial People's Hospital (approval number: 2020183).

Additional information

Correspondence and requests for materials should be addressed to H.A.-B. or C.L.